Original Research

Indoxyl sulfate impairs *in vitro* erythropoiesis by triggering apoptosis and senescence

Thitinat Duangchan[1,2] iD, Manoch Rattanasompattikul[3], Narong Chitchongyingcharoen[1], Sumana Mas-Oodi[1], Moltira Promkan[1], Nuttawut Rongkiettechakorn[3], Suksan Korpraphong[4] and Aungkura Supokawej[1] iD

[1]Department of Clinical Microscopy, Faculty of Medical Technology, Mahidol University, Nakhon Pathom 73170, Thailand; [2]Hematology and Transfusion Science Research Center and School of Allied Health Sciences, Walailak University, Nakhon Si Thammarat 80160, Thailand; [3]Medical Department, Golden Jubilee Medical Center, Faculty of Medicine Siriraj Hospital, Mahidol University, Nakhon Pathom 73170, Thailand; [4]Department of Obstetrics and Gynecology, Police General Hospital, Bangkok 10330, Thailand
Corresponding author: Aungkura Supokawej. Email: aungkura.jer@mahidol.ac.th

Impact Statement

Besides insufficient erythropoietin production due to renal cell damage, uremic toxin retention is a possible cause of anemia in chronic kidney disease (CKD). Therefore, the effects of uremic toxins during erythropoiesis need to be elucidated. In this study, indoxyl sulfate (IS), a protein-bound uremic toxin accumulated in renal disease patients, was administered to CD34+ hematopoietic stem cells during *in vitro* erythropoiesis. Our research found that IS reduced cell proliferation and impaired hematopoietic stem cell differentiation into red blood cells. These findings might result from the triggering of cellular apoptosis and senescence. The treatment of IS induced apoptotic cell death by increasing the expression of apoptotic mRNA markers, loss of nuclear and cell membrane integrity, and DNA fragmentation. Furthermore, the study demonstrated that IS affected cell cycle arrest by upregulating the levels of senescence mRNA markers. These findings could be applied to novel targeted therapy for anemia in CKD.

Abstract

Anemia is a major complication in over 50% of chronic kidney disease (CKD) patients. One of the main causes of anemia in CKD is the reduction of erythropoietin (EPO) synthesis from renal tubular cells. Therefore, first-line treatment of CKD is EPO administration; however, EPO unresponsiveness in several patients is frequently found. More undefined causes of anemia in CKD are under interest, especially uremic toxins, which are a group of solutes accumulated in CKD patients. The highly detectable protein-bound uremic toxin, indoxyl sulfate (IS) was investigated for its effects on *in vitro* erythropoiesis in this study. CD34+ hematopoietic stem cells were isolated from human umbilical cord blood and differentiated toward erythrocyte lineage for 14 days in various concentrations of IS (12.5, 25, 50, and 100 μg/mL). The effects of IS on cell proliferation, differentiation, apoptosis, and senescence were determined. Cell proliferation was investigated by manual cell counting. Cell surface marker expression was analyzed by flow cytometry. Wright's staining was performed to evaluate cell differentiation capacity. Apoptosis and senescence marker expression was measured using reverse transcription polymerase chain reaction (RT-PCR). TUNEL assay was performed to detect apoptotic DNA fragmentation. Our results demonstrated that IS reduced cell proliferation and impaired erythrocyte differentiation capacity. In addition, this study confirmed the effects of IS on cell apoptosis and senescence during erythropoietic differentiation. Therefore, the promotion of apoptosis and senescence might be one of the possible mechanisms caused by uremic toxin accumulation leading to anemia in CKD patients.

Keywords: Uremic toxin, indoxyl sulfate, hematopoietic stem cells, anemia, apoptosis, senescence

Introduction

Chronic kidney disease or CKD is a serious condition that defined as a progressive loss of kidney function over time.[1] The leading reported causes of CKD are from various conditions including diabetes mellitus, hypertension, immunological reactions, glomerulonephritis, and tubule-interstitial fibrosis.[2] CKD patients suffer from fatigue, edema, and anemia.[3] Anemia is a severe complication in CKD, accounting for over 50% of patients with end-stage renal failure.[4] The persistence of anemia in patients with CKD influences the quality of life by long-stay hospitalization, cognitive impairment, increased risk of cardiovascular disease, and mortality.[5,6] The major pathological factor of anemia is the reduction of erythropoietin (EPO) synthesis from interstitial cells residing in the renal cortex. EPO is a hormone mainly produced by kidneys and necessary for red blood cell survival and maturation.[7] Therefore, most CKD patients with anemia are treated with erythropoiesis-stimulating agents (ESAs) such as recombinant EPO.[8] However, the successful outcome of

treatment is dependent on the patient's underlying condition. In addition, the blood EPO level can be considered inappropriately low considering the degree of anemia.[9] These findings indicate that EPO insufficiency may not be the only cause of anemia in CKD. Meanwhile, other factors have been reported to be associated with the pathogenesis of anemia in CKD, for example, hepcidin,[10] hypoxia-inducible factor-1,[11] and uremic toxins.[12]

Uremic toxins are solute substances that originate from cellular metabolism. Many forms of uremic toxins are classified as small water-soluble compounds, low molecular weight compounds, and protein-bound uremic toxins.[13] Indoxyl sulfate (IS), a type of protein-bound uremic toxin, is a metabolic derivative from tryptophan to indole produced by gastrointestinal bacteria. Indole is oxidized and sulfated to form IS in hepatocytes and is normally excreted through the renal proximal tubules.[14] IS can bind with albumin, which causes a high accumulation in CKD patients even when maintaining dialysis.[15] It has been suggested that pathological mechanisms of uremic toxins to promote renal cell damage leading to renal failure include induction of reactive oxygen species (ROS), inflammation, fibrosis, and oxidative stress.[16–18] In addition, uremic toxins have also been reported to cause red blood cell death[19] and neutrophil apoptosis.[20] Moreover, uremic toxin-induced senescence was reported in various kidney cell types, including renal tubular cells, podocytes, endothelial cells, and immune cells.[21–24] However, there is still no study on the apoptosis and senescence effects of IS during erythropoiesis.

In this study, we hypothesized that IS might affect erythrocyte proliferation, differentiation, and maturation, leading to anemia in CKD patients through cellular apoptosis and senescence mechanisms. The study was performed by isolation of CD34+ hematopoietic stem cells from human umbilical cord blood and differentiation toward erythrocyte lineage *in vitro*. The effects of IS were investigated through cell proliferation analysis, differentiation capacity, apoptotic marker investigation, and expression of apoptotic and senescence markers.

Materials and methods

CD34+ mononuclear cell isolation

All umbilical cord blood samples were obtained from full-term deliveries after receiving informed consent according to a protocol approved by Mahidol University Central Institutional Review Board (MU-CIRB 2018/041.0702). Mononuclear cells were isolated from umbilical cord blood using density gradient centrifugation. Briefly, 5 mL of Lymphoprep™ (Alere Technologies AS, Oslo, Norway) was added in a 15-mL conical tube and overlaid with 5 mL of cord blood. Samples were centrifuged at 800 RCF for 20 min at 20°C. The interphase layer was collected and resuspended with 1× phosphate-buffered saline (PBS) containing 2% fetal bovine serum (FBS) (MilliporeSigma, Burlington, MA, USA) and 1 mM EDTA (Fluka Chemie GmbH, Buchs, Switzerland). CD34+ cells were isolated from mononuclear cells by immunomagnetic cell separation using EasySep™ PE Positive Selection Kit (STEMCELL Technologies, Vancouver, Canada). Briefly, 1.5×10^8 cells/mL were added to a round-bottom tube and incubated with 3 μg/mL FcR blocker, 3 μg/mL CD34-PE conjugated antibody (clone no. 8G12), 100 μL/mL selection cocktail, and 50 μL/mL magnetic particles. After incubation, 1× PBS containing 2% FBS and 1 mM EDTA was topped up and placed in an EasySep™ magnetic station for 5 min at room temperature. Isolated CD34+ cells were maintained with Iscove's Modified Dulbecco's Medium (IMDM) (Biochrom GmbH, Berlin, Germany) at 37°C, 5% CO_2 in humidified condition. Purity of CD34+ cells was measured using a FACSCanto™ flow cytometer.

Cell culture

The isolated CD34+ cells were seeded in erythropoietic differentiation medium with or without different concentrations of IS consisting of 12.5, 25, 50, and 100 μg/mL (equivalent to 49.74, 99.48, 198.97, and 397.93 μM, respectively).[25] The erythropoietic differentiation medium containing IMDM supplemented with 3% human AB serum, 2% FBS, 10 μg/mL insulin (Sigma-Aldrich, MO, USA), 3 IU/mL heparin (LEO Pharma, Ballerup, Denmark), 200 μg/mL transferrin (Sigma-Aldrich), 100 IU/mL pen/strep (Life Technologies, CA, USA), and 3 IU/mL EPO (Janssen Pharmaceutica, Beerse, Belgium) was divided into three phases: Phase I (days 0–8) was supplemented with 10 ng/mL stem cell factor (SCF) and 1 ng/mL interleukin 3 (IL3) (both were purchased from STEMCELL Technologies), Phase II (days 9–10) was supplemented with 1 μg/mL SCF, and Phase III (days 11–14) was supplemented with 500 μg/mL transferrin. Erythropoietic differentiation medium supplemented with dimethyl sulfoxide (DMSO) was used as reagent control.

Cell growth analysis

Isolated CD34+ cells (1×10^5 cells) were cultured in erythropoietic differentiation medium with or without IS (0, 12.5, 25, 50, and 100 μg/mL). The media were changed at days 0, 4, 9, and 11. Cell number was manually counted every day for 14 days using a hemocytometer by mixing with trypan blue in the ratio 1:1. The results were plotted on a growth curve.

Cell surface marker analysis

Isolated CD34+ cells (3×10^5 cells) were cultured in erythropoietic differentiation medium with or without IS. Erythropoietic differentiation marker was analyzed at days 4, 7, 11, and 14. Briefly, cells were washed with 1× PBS containing 1 mM EDTA and 2% FBS and centrifuged at 1500 rpm for 5 min at room temperature. Cell pellet was incubated with anti-CD71 APC antibody (clone no. CY1G14) and anti-CD235a FITC antibody (clone no. HI264) (both were purchased from BioLegend, CA, USA) at 4°C for 30 min. After excess antibodies were removed, cells were fixed in 1% paraformaldehyde and investigated using the BD FACSCanto™ II flow cytometer.

Differentiated cell morphology analysis

The morphology of erythropoietic differentiation was investigated at days 4, 7, 11, and 14 after cultivation with erythropoietic differentiation medium with or without IS. Briefly, cells were washed with 1× PBS and resuspended in 5 μL

human albumin (Plasma Fractionation Center, The Thai Red Cross Society, Chonburi, Thailand) and smeared on glass slides. Slides were air-dried 5–10 min and fixed with absolute methanol (Honeywell, Charlotte, NC, USA). After methanol was evaporated, slides were incubated with Wright's stain for 3 min, and Wright's stain buffer added for 4 min. Slides were rinsed with running water and air-dried. Cell morphology was determined and counted using a light microscope (Olympus, Shinjuku, Tokyo, Japan).[26]

Annexin V–PI assay

Cells were harvested at days 7 and 14 after erythropoietic differentiation to perform Annexin V–PI staining (BD Biosciences, CA, USA). Briefly, 1×10^5 cells were collected and washed twice with $1\times$ PBS. Cells were resuspended with 100 µL of $1\times$ binding buffer containing 0.1 M Hepes (pH 7.4), 25 mM $CaCl_2$, and 1.4 M NaCl. Annexin V-FITC conjugated and PI were added and incubated at room temperature for 15 min in the dark.[27] Binding buffer was added to the sample prior to analysis with FACSCanto II flow cytometry. FlowJo software (version 10.6.2) was used to analyze the data.

RNA extraction and quantitative reverse transcription polymerase chain reaction analysis

Cells were collected in Trizol® reagent (Thermo Fisher Scientific, MA, USA) and extracted RNA using Direct-zol™ RNA MiniPrep (ZYMO Research, CA, USA). The concentration and purity of RNA were quantified using the NanoDrop™ spectrophotometer and NanoDrop™ 2000 software (Thermo Fisher Scientific). cDNA template was synthesized using the Revert Aid First Strand cDNA synthesis kit (Thermo Fisher Scientific). Quantitative reverse transcription polymerase chain reaction (qRT-PCR) was performed using SYBR® FAST qPCR Master Mix (Kapa Biosystems/Roche Holding AG, Switzerland). Briefly, cDNA template was mixed with $2\times$ KAPA SYBR master mix, forward and reverse primers and distilled water. The PCR reaction was performed for 40 cycles of enzyme inactivating at 95°C for 3 min, denaturing at 95°C for 3 s, annealing at 60°C for 30 s and extension at 72°C for 20 s using a CFX96 machine. Relative gene expression was evaluated using the $2^{-\Delta\Delta ct}$ method after normalization to the reference gene.[28] All primers are listed in Supplementary Table S1.

TUNEL assay

Cell death was analyzed using the TUNEL assay provided by the In Situ Cell Death Detection Kit, Fluorescein (Roche Holding AG) according to the manufacturer's instructions. First, cells were collected and fixed in 4% paraformaldehyde in PBS pH 7.4 for 1 h at room temperature. After rinsing with $1\times$ PBS, cells were permeabilized with 0.1% Triton X-100 in 0.1% sodium citrate for 2 min. Thereafter, samples were rinsed twice with $1\times$ PBS and incubated with 50 µl of TUNEL reaction mixture at 37°C for an hour in the dark. Next, samples were rinsed three times with $1\times$ PBS and counterstained with ProLong™ Gold Antifade Mountant with DAPI. Cell death was analyzed using a fluorescence microscope. A minimum of 1000 cells were counted in five different fields and calculated the percentage of TUNEL-positive cells.

Cell senescence analysis

Cell senescence analysis was performed using the Senescence β-Galactosidase (β-gal) Staining Kit (Cell Signaling Technology, MA, USA) following the manufacturer's instructions. Briefly, cells were collected in a 1.5-mL microtube and washed with $1\times$ PBS. Cells were fixed with $1\times$ fixative solution for 15 min at room temperature and rinsed twice with $1\times$ PBS. Cells were then incubated with β-gal staining solution at 37°C overnight. Stained cells were dropped on glass slides and covered with a coverslip. Cell senescence was analyzed using a light microscope.

Statistical analysis

All data are presented as the mean value ± standard error of the mean (SEM) from at least three independent experiments. Statistical analysis was investigated using GraphPad Prism software (version 6.01; GraphPad Software, CA, USA). A one-way analysis of variance (ANOVA) with Tukey's post hoc test was used to analyze the differences among groups. Statistical significance was considered at P value < 0.05.

Results

IS reduces cell growth during erythrocyte differentiation

Cells isolated from umbilical cord blood mononuclear cells by magnetic cell sorting were quantified for the number of CD34+ population. Flow cytometry analysis indicated that of CD34+ cells was increased from $2.33 \pm 1.35\%$ (presort) to $84.04 \pm 8.50\%$ (postsort) (Figure 1(a) and (b)). These cells were used to investigate the effect of IS on *in vitro* erythropoiesis by culturing in differentiation medium in the presence and absence of IS for 14 days (Figure 1(c)). The results demonstrated that the cell number in all conditions increased 13–15 folds from the initial cells at day 5 and reached the maximum growth at day 14. The number of cells in IS treatment groups was significantly reduced compared to control groups after day 7. At the end of differentiation phase, the cumulative cell numbers of CTRL, DMSO, 12.5, 25, 50, and 100 µg/mL IS were $25.6 \times 10^5 \pm 5.6 \times 10^5$, $24.0 \times 10^5 \pm 4.2 \times 10^5$, $10.3 \times 10^5 \pm 6.6 \times 10^5$, $10.8 \times 10^5 \pm 7.0 \times 10^5$, $8.3 \times 10^5 \pm 4.9 \times 10^5$, and $4.4 \times 10^5 \pm 1.1 \times 10^5$ cells, respectively (Figure 2 and Table S2).

IS impairs *in vitro* erythrocyte differentiation

During *in vitro* erythrocyte differentiation with the treatment of IS (0, 12.5, 25, and 50 µg/mL), erythropoietic cell surface markers (CD71 and CD235a) and morphology were investigated at days 4, 7, 11, and 14. The CD71⁻/CD235a⁻ subpopulation was identified as undifferentiated cells, while CD71⁺/CD235a⁻ and CD71⁺/CD235a⁺ showed early and late premature erythrocyte differentiation, and the CD71⁻/CD235a⁺ subpopulation represented mature erythrocytes (Figure 3(a) to (d)). At day 4, erythrocyte marker expression in the control and IS-treated groups was not different.
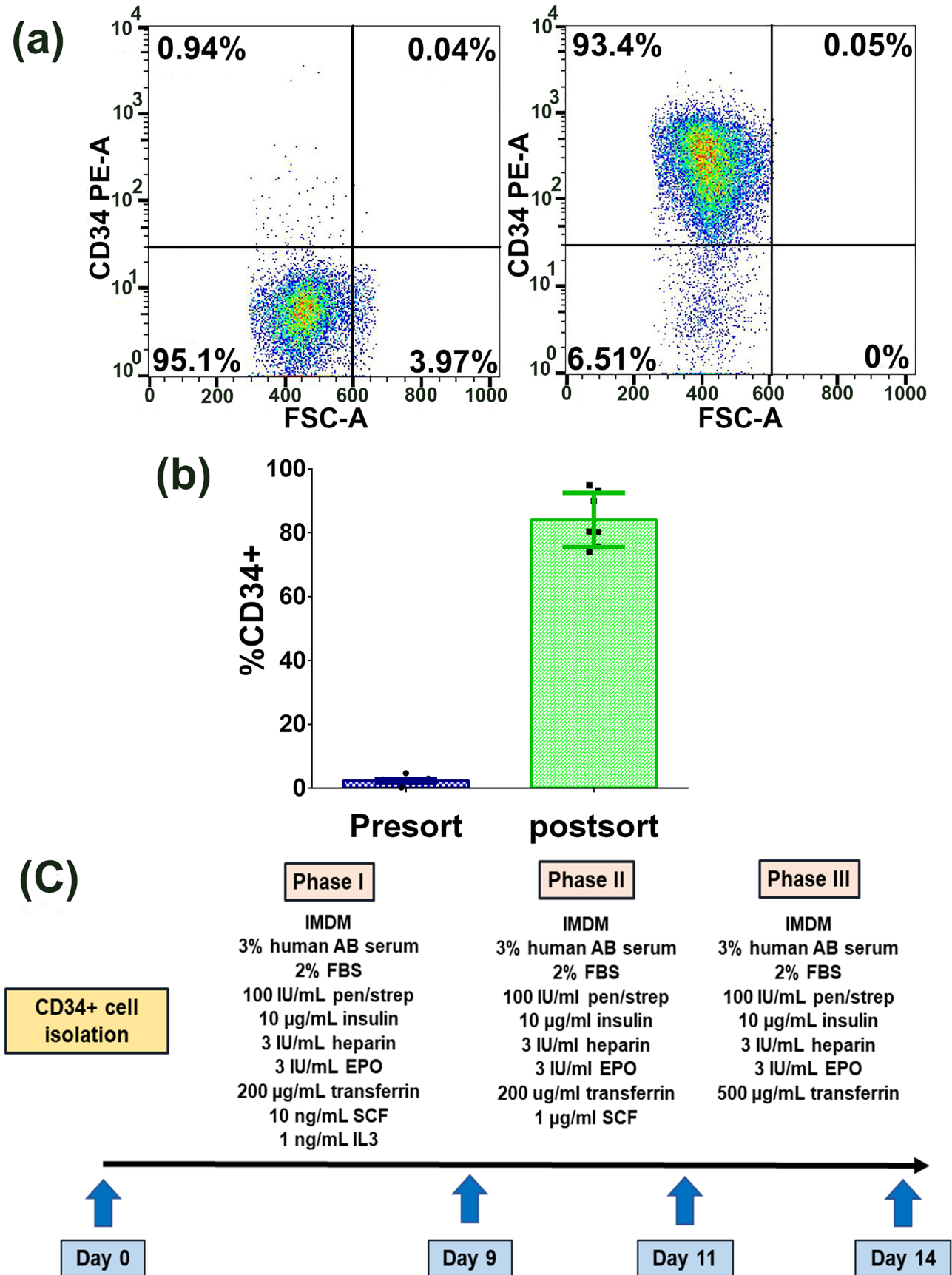
Figure 1. CD34+ cell isolation and erythrocyte differentiation procedure. (a) Umbilical cord blood mononuclear cells were analyzed for the purity of CD34+ cells before magnetic cell sorting (presort) and after sorting (postsort). (b) Quantitative measurement of umbilical cord mononuclear cells demonstrated a higher amount of CD34+ cells after sorting (84.04 ± 8.50%) compared to presort (2.33 ± 1.35%). Data are shown as mean value ± SD ($n = 7$). (c) CD34+ cells were differentiated to erythrocytes by culturing in three phases of differentiation medium for 14 days in combination with IS at concentrations of 12.5, 25, 50, and 100 µg/mL. (A color version of this figure is available in the online journal.)
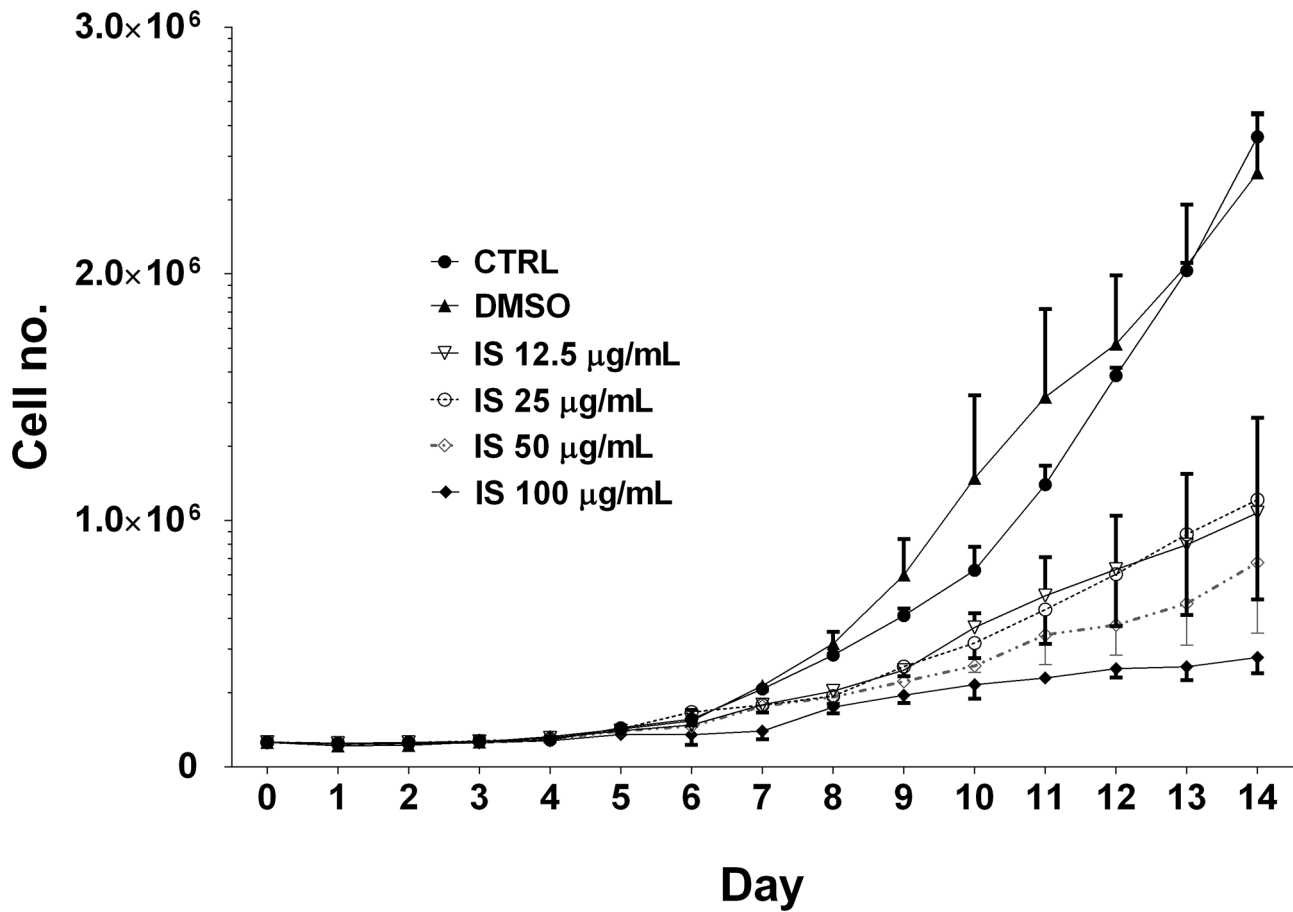
Figure 2. Cell growth analysis. Cell number of CD34+ cells during erythrocyte differentiation was counted and presented as a growth curve. Three independent experiments were analyzed and presented as mean value ± SEM. One-way ANOVA was used as a statistical analysis. $P < 0.05$ was identified as a significant difference.

Most erythropoietic cells under IS treatment remained in an undifferentiated state (CD71⁻/CD235a⁻) at days 7 and 11. However, IS treatment showed a significantly lower number of later state differentiations (CD71⁺CD235a⁻ and CD71⁺/CD235a⁺) at days 7, 11, and 14 (Figure 4(a) to (d)). We further investigated erythrocyte differentiation using a morphological study. Erythropoiesis stages – comprising pronormoblast, basophilic normoblast, polychromatic normoblast, orthochromatic normoblast, and mature erythrocyte – were identified by Wright's stain (Figure 5(a)) and are presented as a percentage (Figure 5(b)). However, the morphological study did not show significant changes after IS treatment compared to the CTRL group.

IS increases cellular apoptosis during *in vitro* erythropoiesis

One of the possible mechanisms which might lead to the reduction of cell number and impairment of differentiation is apoptosis. FITC-conjugated Annexin V and PI staining was performed to investigate apoptotic cell death. Flow cytometry analysis revealed the population of live cells (Annexin V⁻/PI⁻), early apoptosis (Annexin V⁺/PI⁻), late apoptosis (Annexin V⁺/PI⁺), and necrosis (Annexin V⁻/PI⁺) (Figure 6(a) and (b)). During *in vitro* erythropoiesis, cells with IS treatment exhibited an increased apoptotic rate in a

dose-dependent manner at day 14 and showed a significant increase in the 50 and 100 µg/mL treated groups (Figure 7). DNA fragmentation, the hallmark of late stage apoptosis, was further investigated using TUNEL assay to stain 3′-hydroxyl termini in the double-strand DNA breaks at day 14 of the treatment (Figure 8(a)). IS-treated cells showed increased TUNEL-positive cells in a dose-dependent manner, and this significantly increased in the 25, 50, and 100 µg/mL IS treatment groups (Figure 8(b)). The expression of apoptotic markers (*BAX* and *BID*) was investigated using quantitative RT-PCR analysis. The results revealed that the expression of proapoptotic genes tended to increase in cells treated with IS. In addition, a significant increase of *BAX* expression was found at day 7 in the 12.5 µg/mL IS treatment group (Figure 9(a) and (b)).

IS induces cellular senescence

The effect of IS on cellular senescence was also investigated using real-time qRT-PCR. The senescence markers – including P16, P21, and P53 – play a major role in cell cycle arrest which is a hallmark of cellular senescence. The results indicated that the mRNA expression of *P16* and *P21* were significantly upregulated under 100 µg/mL IS at day 7 (Figure 10(a) and (b)). Similarly, 100 µg/mL of IS significantly increased *P53* mRNA expression at days 7 and 14 (Figure 10(c)).
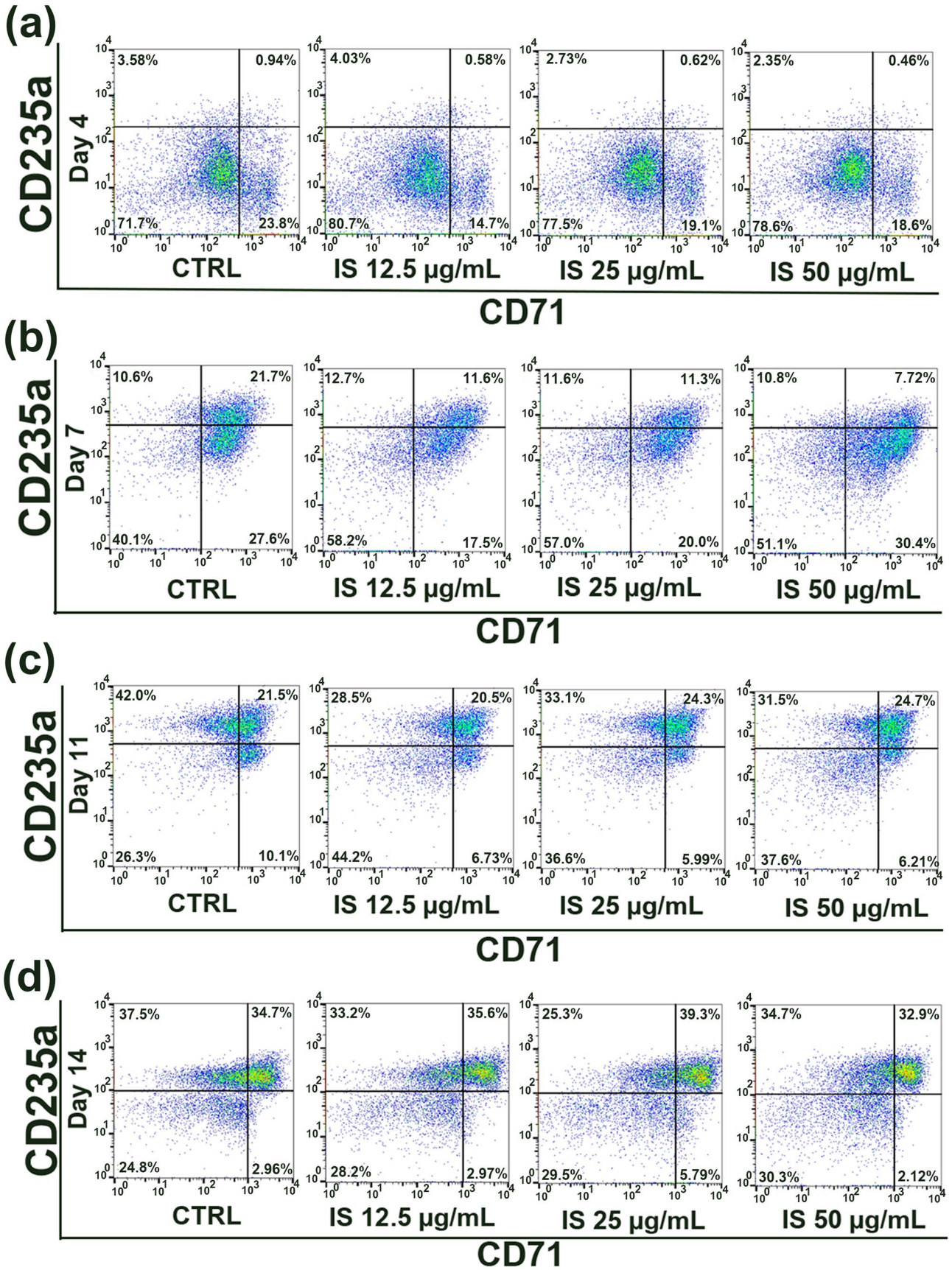
Figure 3. CD marker expression of *in vitro* erythrocyte differentiation. Erythrocyte subpopulation was evaluated by determination of CD71 and CD235 expression using flow cytometry after differentiation for 4 (a), 7 (b), 11 (c), and 14 days (d). (A color version of this figure is available in the online journal.)
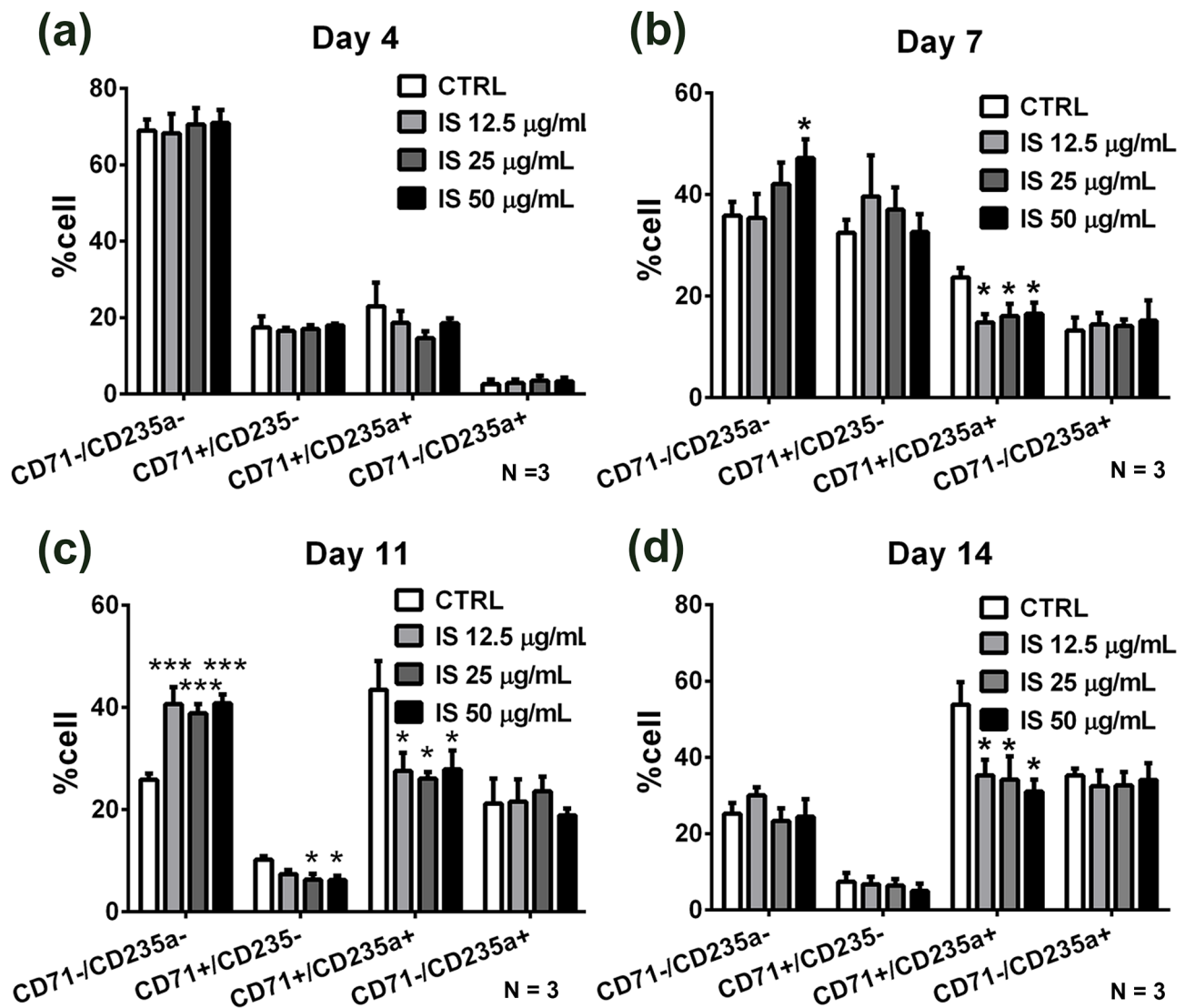
Figure 4. Quantitative expression of erythrocyte differentiation markers. The quantitative measurement of CD71⁻/CD235a⁻, CD71⁺/CD235a⁻, CD71⁺/CD235a⁺, and CD71⁻/CD235a⁺ was investigated. (a) At day 4, there was no significant change in erythrocyte marker expression. (b) At day 7, IS treatment with 50 μg/mL showed significantly higher cell number in undifferentiated population, CD71⁻/CD235a⁻ ($P = 0.0458$), whereas cell number of IS treatment groups decreased in later differentiation marker, CD71⁺/CD235a⁺ ($P = 0.0157$ in 12.5 μg/mL, 0.0302 in 25 μg/mL, and 0.0395 in 50 μg/mL). (c) At day 11, IS demonstrated a higher number of undifferentiated cells ($P = 0.0002$ in 12.5 μg/mL, 0.0002 in 25 μg/mL, and 0.0001 in 50 μg/mL), while showing a reduced level of CD71⁺/CD235a⁻ ($P = 0.0128$ in 25 μg/mL and 0.012 in 50 μg/mL), and CD71⁺/CD235a⁺ ($P = 0.0197$ in 25 μg/mL, 0.0131 in 25 μg/mL and 0.0214 in 50 μg/mL). (d) At day 14, the treatment of IS was significantly decreased CD71⁺/CD235a⁺ ($P = 0.0294$ in 12.5 μg/mL, 0.023 in 25 μg/mL, and 0.0116 in 50 μg/mL). One-way ANOVA was used as a statistical analysis. $P < 0.05$ was identified as a significant difference.
*$P < 0.05$; ***$P < 0.001$ vs CTRL.

Senescence-associated β-gal can be used as a biomarker of senescence. So, we further investigated β-gal staining of IS-treated cells at day 14. As shown in Figure S1, the β-gal positive cells were increased in IS-treated cells compared to control groups.

Discussion

IS is a low molecular weight metabolite of dietary tryptophan and easily binds to the albumin called protein-bound uremic toxin. In CKD patients with impaired kidney function or end-stage kidney disease, IS cannot be removed even with hemodialysis treatment and subsequently accumulates in the blood circulation.[29] Chih-Jen Wu demonstrated that both free and total IS significantly reduced the EPO level by inhibiting EPO expression and decreasing plasma EPO concentrations.[30] Several studies have demonstrated the strong toxicities of protein-bound uremic toxins that are associated with systemic disorders, including cardiovascular disease, bone and mineral disorders as well as anemia.[13,31] The increased removal of protein-bound uremic toxins might constitute a basic approach to improve clinical outcomes.[32] The study of *in vitro* IS effects should consider the interaction between IS and albumin, including the acceptable concentration used and other factors that affect IS-albumin binding capacity.[33] The IS level in 103 CKD patients was determined and its alteration was associated with the stage of CKD; Stage 3: 3.2 ± 3.0 μg/mL, Stage 4: 5.4 ± 3.6 μg/mL, Stage 5: 19.9 ± 10.5 μg/mL, and Stage 5 with hemodialysis: 42.5 ± 15.6 μg/mL.[34] Furthermore, another study
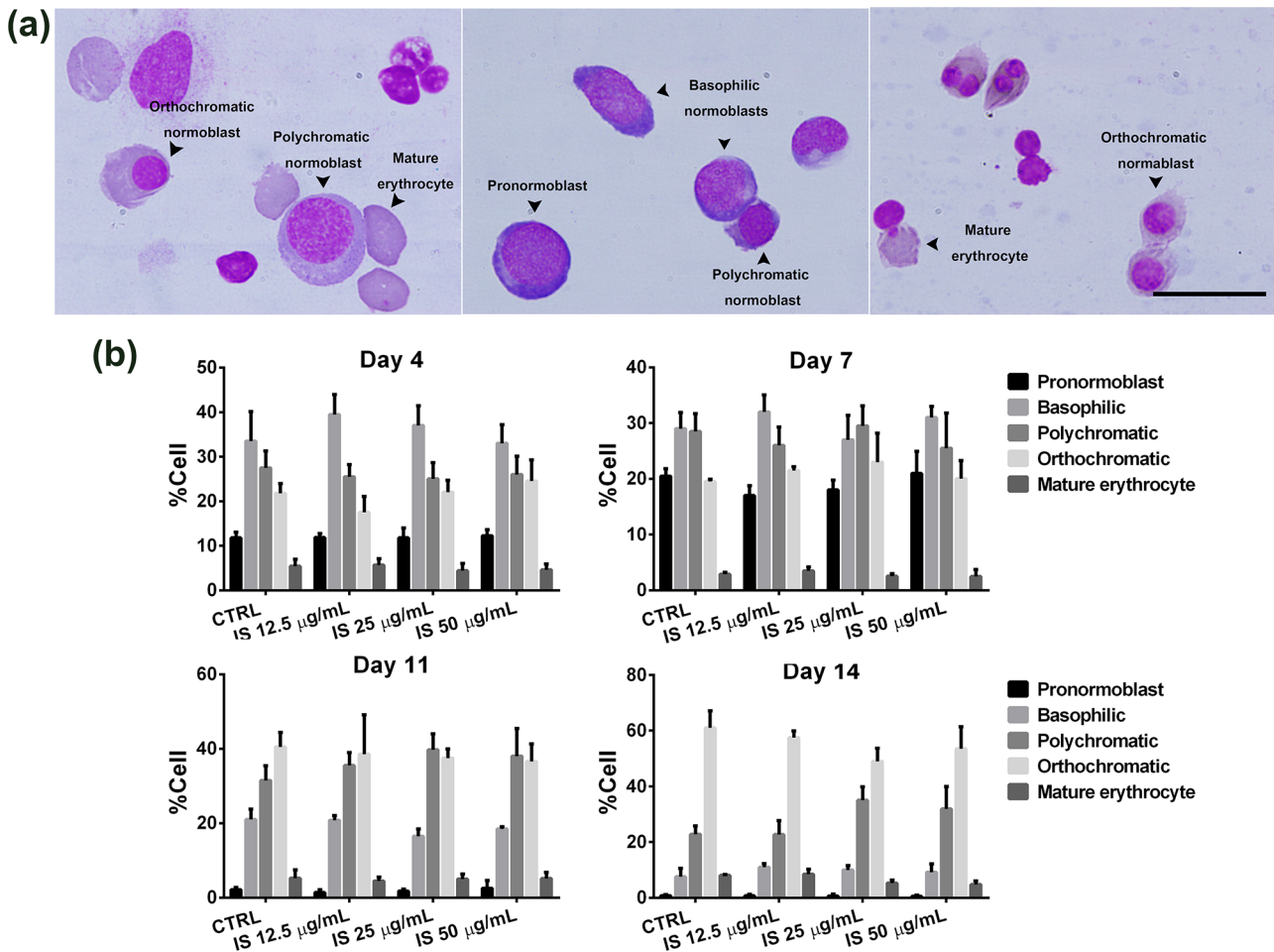
Figure 5. Wright's staining of *in vitro* erythrocyte differentiation. (a) Erythrocyte differentiation morphology was evaluated using Wright's stain. Scale bar 50 µm. (b) Quantitative measurement of erythropoiesis stages showed no significant difference after IS treatment for 4, 7, 11, and 14 days. The data are shown as mean value ± SEM (*n* = 3). One-way ANOVA was used as a statistical analysis. *P* < 0.05 was identified as a significant difference compared to control. (A color version of this figure is available in the online journal.)

demonstrated that the baseline level of IS in 1170 hemodialysis patients was 31.6 µg/mL and the maximum concentration was 102.2 µg/mL.[35] However, there is no evidence of IS pathological concentration that affects *in vitro* erythropoiesis. The previous study reported that mature red blood cells from healthy donors treated with IS at concentrations of 90 µM (23.6 µg/mL) and 170 µM (42.7 µg/mL) increased ROS production and cell death.[36] Therefore, the IS concentrations used in this study (0, 12.5, 25, 50, and 100 µg/mL) are correlated with CKD physiological concentration and might be used as CKD pathological concentration for investigation of erythropoiesis *in vitro*.

Recently, stem cell-based models are becoming powerful tools for pathogenesis study in various diseases resulting from genetic risks and environmental factors due to their self-renewal and differentiation properties.[37,38] The *in vitro* erythropoiesis assay is a promising strategy for examining red blood cell development and disease-related red blood cell abnormality. In this study, the erythroid cells were derived from cord blood of healthy donors with a differentiation protocol and the exposure of cells to various concentrations of IS mimicked CKD patients. The hematopoietic stem cell isolation and erythrocyte differentiation

procedure were adapted from the previous reports.[39,40] The differentiation medium contains several cytokines, including heparin and insulin, which are responsible for stem cell proliferation, hematopoiesis, and differentiation. However, both heparin and insulin did not affect in cell number during hematopoietic stem cell differentiation through erythroid cells.[40] In addition, the proliferation rate might be affected by DMSO, which is used as a solvent of IS. Therefore, besides control group, we evaluated the proliferation of treated cells with the same concentration of DMSO as a reagent control and the culture medium was freshly prepared before use. Our findings revealed that the treatment of IS decreased cell proliferation rate and impaired *in vitro* erythropoietic differentiation capacity. During erythropoiesis, erythrocyte development was delayed, with cells being retained in the early stage and a low cell number advancing to the late stage of erythropoiesis differentiation. In previous studies, uremic toxins, polyamines, were shown to reduce erythroid colony formation (CFU-E) and erythroid maturation by inhibition of EPO activity.[41–43] In addition, Mathias *et al.*[44] demonstrated that the reduction of CD34+ cell expansion and cell viability, especially in the polychromatic normoblast stage during *in vitro* erythropoiesis resulted from apoptotic cell death.
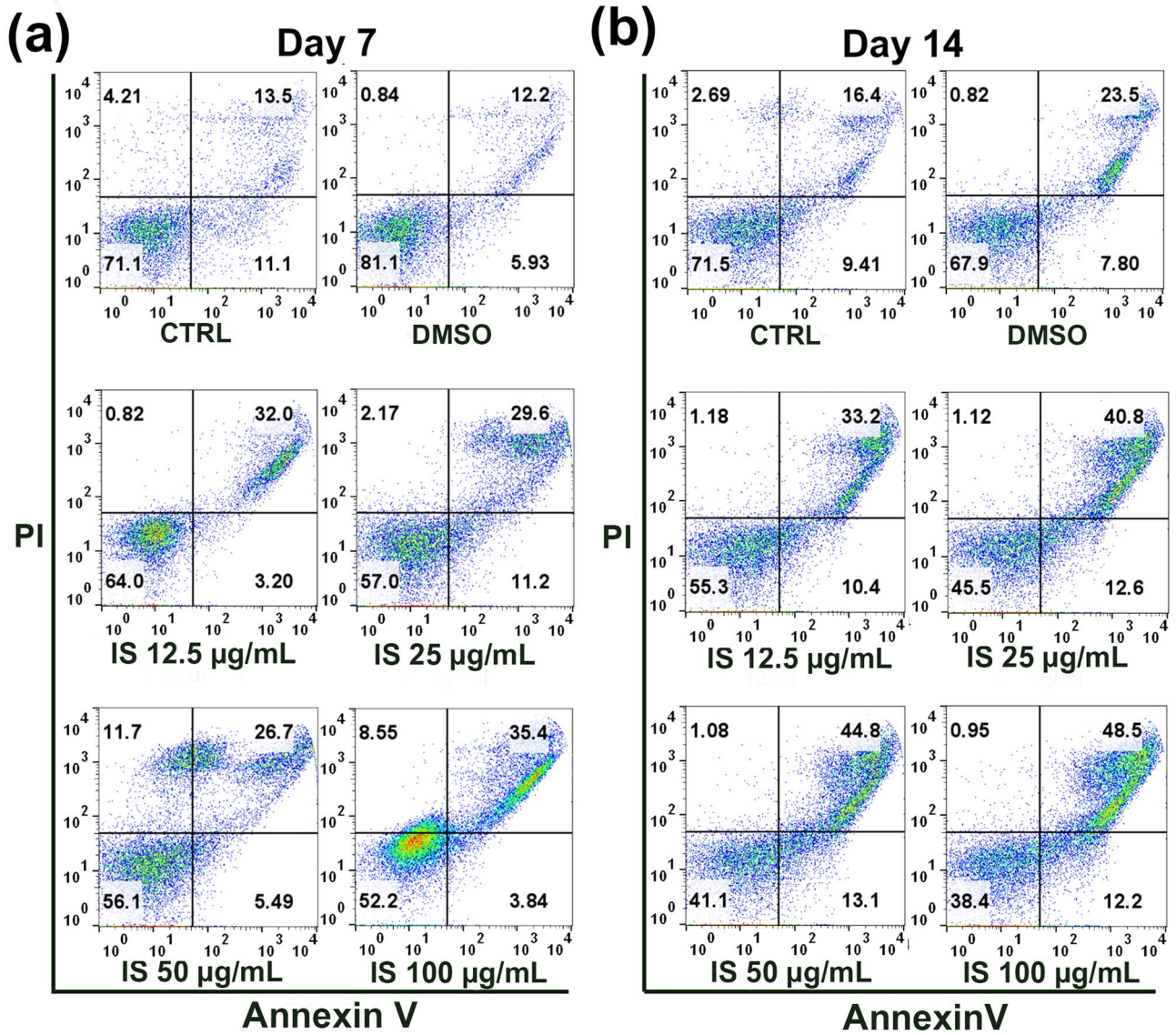
Figure 6. Annexin V–PI staining analysis. Apoptotic cell death during erythrocyte differentiation was analyzed by Annexin V–PI staining using flow cytometry at days 7 (a) and 14 (b). (A color version of this figure is available in the online journal.)
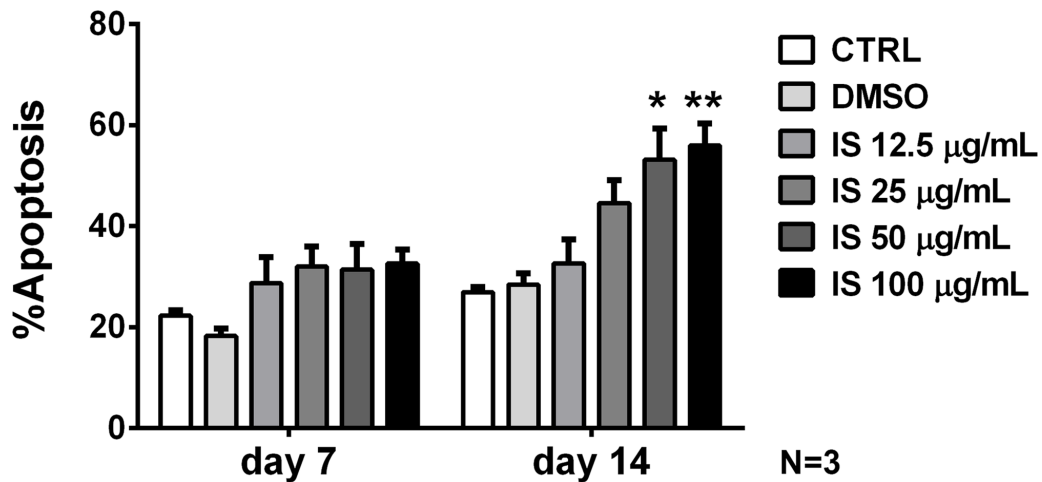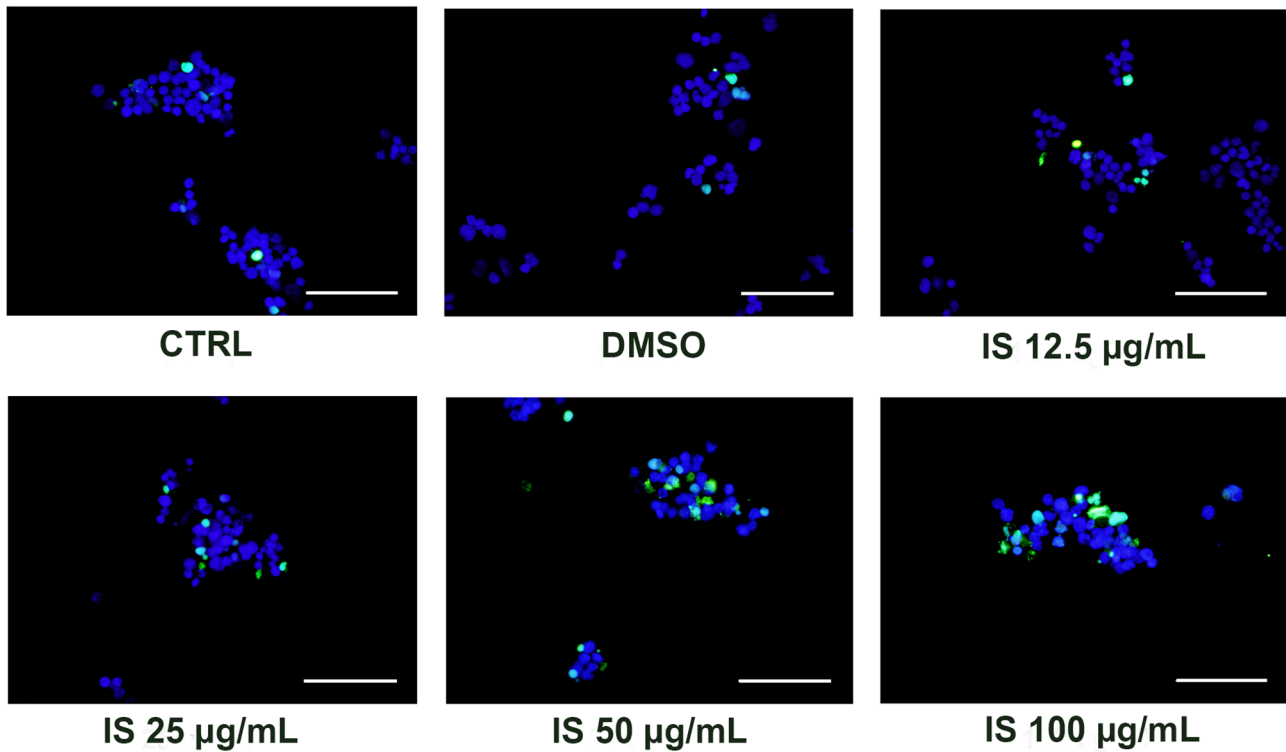

Figure 7. Quantitative analysis Annexin V–PI staining. Apoptotic cell death was significantly increased at day 14 in 50 µg/mL ($P = 0.0114$) and 100 µg/mL ($P = 0.0054$). One-way ANOVA was used as a statistical analysis. $P < 0.05$ was identified as a significant difference. *$P < 0.05$; **$P < 0.01$ vs CTRL.
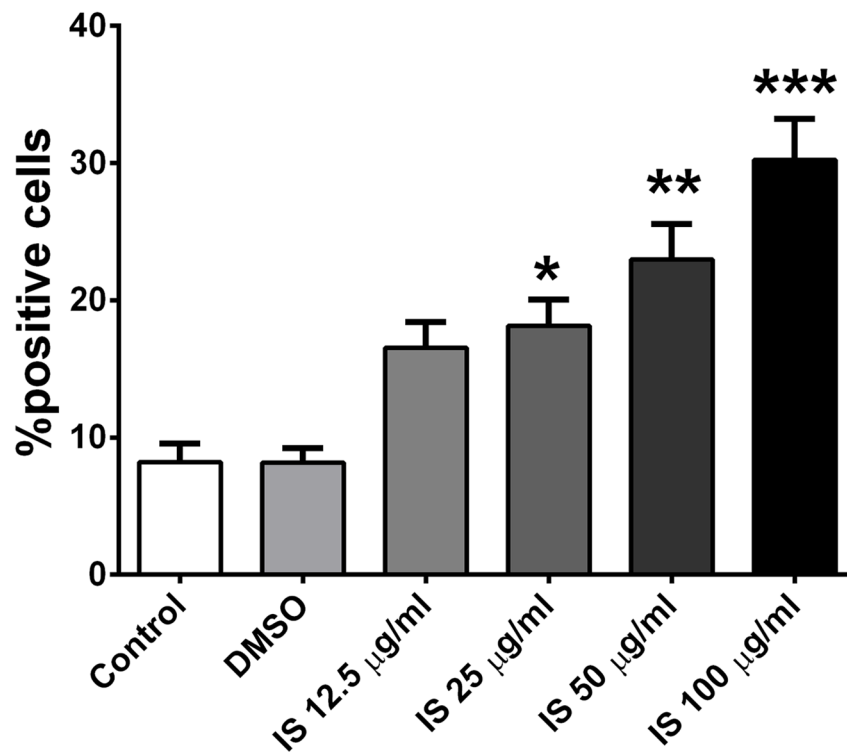
Figure 8. TUNEL assay analysis. (a) DNA fragmentation during apoptosis was analyzed by TUNEL assay at day 14. TUNEL-positive cells are shown as green dots. DAPI was used as the counterstain (blue). Scale bar 50 μm. (b) IS treatment significantly increased TUNEL-positive cells in 25 μg/mL ($P = 0.048$), 50 μg/mL ($P = 0.0031$), and 100 μg/mL ($P < 0.0001$). One-way ANOVA was used as a statistical analysis. $P < 0.05$ was identified as a significant difference. (A color version of this figure is available in the online journal.)
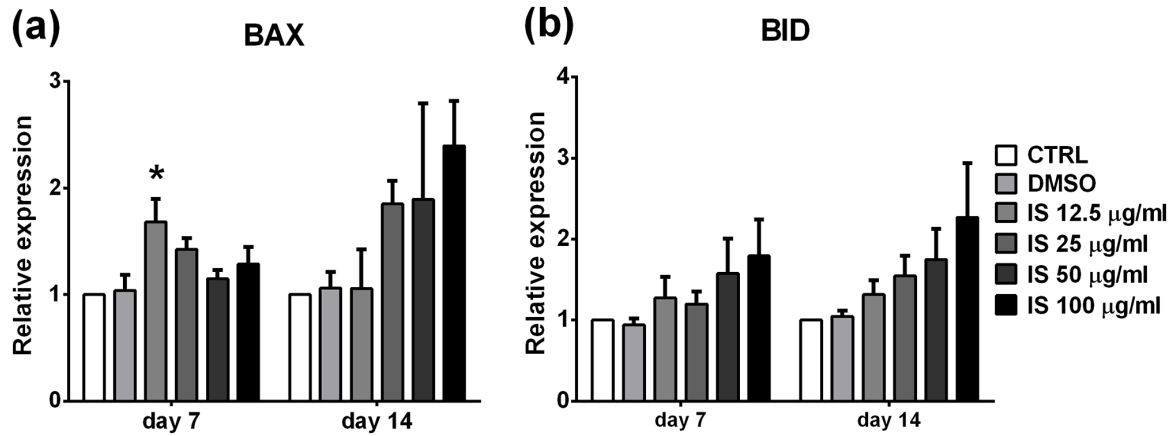*$P < 0.05$; **$P < 0.01$; ***$P < 0.001$ vs CTRL.

Figure 9. qRT-PCR analysis of apoptotic markers. (a) The expression of *BAX* was significantly increased in IS treatment with the concentration of 12.5 µg/mL at day 7 ($P = 0.0454$). (b) The levels of BID were upregulated in IS treatment but not significantly different. Data are shown as mean value ± SEM ($n = 3$). One-way ANOVA was used as a statistical analysis. $P < 0.05$ was identified as a significant difference.
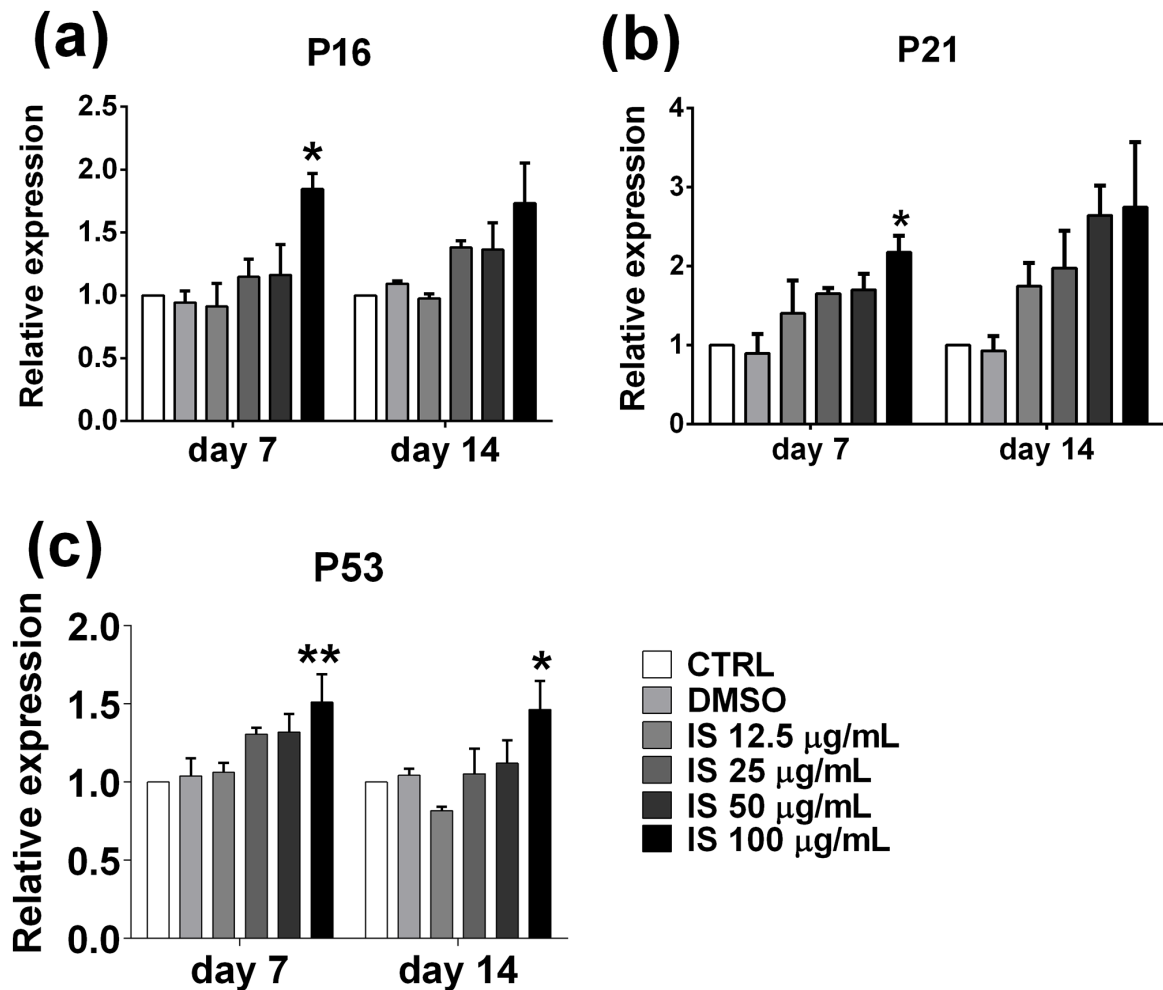*$P < 0.05$ vs CTRL.

Figure 10. qRT-PCR analysis of senescence markers. (a) *P16* expression was significantly upregulated in 100 µg/mL IS treatment at day 7 ($P = 0.0174$). (b) The level of *P21* expression was significantly increased in 100 µg/mL of IS ($P = 0.0351$) at day 7. (c) The expression of *P53* was statistically upregulated in 100 µg/mL of IS at day 7 ($P = 0.0084$) and day 14 ($P = 0.0444$). Data are shown as mean value ± SEM ($n = 3$). One-way ANOVA was used as a statistical analysis. $P < 0.05$ was identified as a significant difference.
*$P < 0.05$; **$P < 0.01$ vs CTRL.

Mature red blood cells circulate in the bloodstream for more than 100 days. However, the acceleration of red blood cell death contributes to anemia characterized by cell shrinkage and being engulfed by macrophages.[45] Several uremic toxins have been identified to cause suicidal red blood cell death (eryptosis), such as acrolein, methylglyoxol, vanadate, and IS.[19,46–48] In this study, the results of Annexin V–PI staining showed the exposure of cell membrane phosphatidylserine indicating that IS induced cellular apoptosis during *in vitro* erythrocyte differentiation. Furthermore, DNA fragmentation, the hallmark of apoptosis, was confirmed by the TUNEL assay. Bcl-2 family proteins play a major role in apoptotic pathways, and they can be divided into three groups composing of pro-apoptotic BH3-only proteins (Bid), pro-survival Bcl-2-like proteins (Mcl-1 and Bcl-2), and pore-forming proteins (Bak and Bax).[49,50] The pro-apoptotic Bid is activated by caspase-8 and directly binds to Bax. Activated Bax oligomerizes to form pores in the mitochondrial outer membrane that releases cytochrome to initiate apoptotic cell death.[51] In this study, qRT-PCR results demonstrated that IS promoted *BAX* mRNA expression.

Senescence is a cell cycle arrest mechanism identified by loss of cell proliferation capacity.[52] The previous studies reported that senescence impaired mesenchymal stem cell proliferation and differentiation capacity.[53,54] Cellular senescence can be triggered by various stress inducers including oxidative stress, DNA damage, and oncogene activation. Cell cycle arrest is controlled by several signaling molecules, including P53, P21, and P16. P53 is a transcription factor, which directly regulates the expression of P21.[55] In addition, these senescence proteins function to inactivate Rb and promote cell cycle arrest.[56,57] Recently, we found that IS treatment triggered cell senescence during erythropoiesis by upregulating P53 expression that consequently triggered the expression of P21 leading to a promotion of the P53/P21 axis of cellular senescence. Furthermore, this study showed that P16 expression was also significantly upregulated. The increased expression of β-gal was detected in the cells treated with IS. However, more samples should be investigated to support the senescence mechanism of IS. In addition, other senescence markers should be further studied, such as telomere length, lamin B1 downregulation, senescence-associated secretory phenotype (SASP), and ROS production.[56] Previously, several studies have demonstrated that IS induced senescence by increased ROS production and upregulated senescence markers in various cell types including proximal tubular cells,[23] endothelial cells,[58] and vascular smooth cells.[59]

The study of IS effects in mature erythrocytes demonstrated that IS treatment induced the level of ROS production and increased red blood cell death. The organic anion transporter 2 (OAT2) in the red blood cell (RBC) membrane plays a major role in IS uptake with NADPH oxidase activity-dependent mechanism.[36] IS induced eryptosis by enhancing extracellular Ca^{2+} influx resulting to cell shrinkage and membrane scrambling.[19] There are several studies suggesting that uremic toxins are associated with apoptosis in various hematopoietic cells in CKD patients, including polymorphonuclear cells,[60] monocytes,[61] neutrophils,[62] lymphocytes,[63] and platelets.[64] In addition, Thomas Crépin et al. reported the shortening of telomere length and reduced lymphocyte count of peripheral blood mononuclear cells (PBMCs) derived from CKD patients, which were associated with senescence.[65] The example of ineffective erythropoiesis as the pathological cause of the disease is thalassemia, which is presented by the increase of ROS in the red cell precursors.[66] The activation of macrophages in bone marrow of β-thalassemia patients indicated the apoptosis and senescence of erythroid progenitor cells.[67]

In conclusion, this study has revealed the pathogenic effects of protein-bound uremic toxin, IS, during *in vitro* erythropoiesis. IS treatment reduced cell proliferation and impaired erythrocyte differentiation capacity. These abnormality conditions might partly be due to two mechanisms – apoptosis and senescence. Therefore, the promotion of apoptosis cell death and cellular senescence during erythrocyte differentiation might be one of the possible mechanisms caused by uremic toxin accumulation leading to anemia in CKD patients. However, this study has some limitations due to the lack of the information from patient's own cells, and there are no any other reports that describe the effects of uremic toxins in senescence and apoptosis during the differentiation of hematopoietic stem cells to red blood cell lineage by *in vivo* animal model. Therefore, the study of IS mechanism causing anemia in CKD patients is needed to be further elucidated using the erythroid progenitor cells from CKD patients and animal-based models that would be the promising approaches to support our findings.

AUTHORS' CONTRIBUTIONS

T.D. performed the experiments and wrote the manuscript. M.R. wrote the manuscript. N.C. performed the experiments. S.M. and M.P. analyzed the results. N.R. designed the study. S.K. provided the samples. A.S. designed the study, reviewed and, edited the manuscript. All authors have reviewed and approved the manuscript.

DECLARATION OF CONFLICTING INTERESTS

The author(s) declared no potential conflicts of interest with respect to the research, authorship, and/or publication of this article.

ETHICAL APPROVAL

The experiment protocol was approved by Mahidol University Central Institutional Review Board (MU-CIRB 2018/041.0702). Written informed consent was obtained from healthy, full-term pregnant Thai women (aged between 23 and 35 years, average 29.84 years old). All experiments were carried out in accordance with relevant guidelines and regulations.

ORCID IDS

Thitinat Duangchan (iD) https://orcid.org/0000-0002-7404-6664
Aungkura Supokawej (iD) https://orcid.org/0000-0002-3979-873X

REFERENCES

1. Levey AS, Eckardt K-U, Tsukamoto Y, Levin A, Coresh J, Rossert J, De Zeeuw D, Hostetter TH, Lameire N, Eknoyan G. Definition and classification of chronic kidney disease: a position statement from Kidney Disease: Improving Global Outcomes (KDIGO). *Kidney Int* 2005;**67**: 2089–100

2. Matovinović MS. 1. Pathophysiology and classification of kidney diseases. *EJIFCC* 2009;**20**:2–11

3. Mehdi U, Toto RD. Anemia, diabetes, and chronic kidney disease. *Diabetes Care* 2009;**32**:1320–6

4. Stauffer ME, Fan T. Prevalence of anemia in chronic kidney disease in the United States. *PLoS ONE* 2014;**9**:e84943

5. Babitt JL, Lin HY. Mechanisms of anemia in CKD. *J Am Soc Nephrol* 2012;**23**:1631–4

6. Liabeuf S, Cheddani L, Massy ZA. Uremic toxins and clinical outcomes: the impact of kidney transplantation. *Toxins* 2018;**10**:229–46

7. Jelkmann W. Regulation of erythropoietin production. *J Physiol* 2011;**589**:1251–8

8. Vázquez-Méndez E, Gutiérrez-Mercado Y, Mendieta-Condado E, Gálvez-Gastélum FJ, Esquivel-Solís H, Sánchez-Toscano Y, Morales-Martínez C, Canales-Aguirre AA, Márquez-Aguirre AL. Recombinant erythropoietin provides protection against renal fibrosis in adenine-induced chronic kidney disease. *Mediators Inflamm* 2020;**2020**:8937657

9. Mercadal L, Metzger M, Casadevall N, Haymann JP, Karras A, Boffa JJ, Flamant M, Vrtovsnik F, Stengel B, Froissart M, NephroTest Study Group. Timing and determinants of erythropoietin deficiency in chronic kidney disease. *Clin J Am Soc Nephrol* 2012;**7**:35–42

10. Nakanishi T, Kimura T, Kuragano T. The hepcidin-anemia axis: pathogenesis of anemia in chronic kidney disease. *Contrib Nephrol* 2019;**198**:124–34

11. Kaplan JM, Sharma N, Dikdan S. Hypoxia-inducible factor and its role in the management of anemia in chronic kidney disease. *Int J Mol Sci* 2018;**19**:389–409

12. Macdougall IC. Role of uremic toxins in exacerbating anemia in renal failure. *Kidney Int Suppl* 2001;**78**:S67–72

13. Lisowska-Myjak B. Uremic toxins and their effects on multiple organ systems. *Nephron Clin Pract* 2014;**128**:303–11

14. Leong SC, Sirich TL. Indoxyl sulfate-review of toxicity and therapeutic strategies. *Toxins* 2016;**8**:358–70

15. Morimoto K, Tominaga Y, Agatsuma Y, Miyamoto M, Kashiwagura S, Takahashi A, Sano Y, Yano K, Kakinuma C, Ogihara T, Tomita M. Intestinal secretion of indoxyl sulfate as a possible compensatory excretion pathway in chronic kidney disease. *Biopharm Drug Dispos* 2018;**39**:328–34

16. Lisowska-Myjak B. Serum and urinary biomarkers of acute kidney injury. *Blood Purif* 2010;**29**:357–65

17. Satoh M, Hayashi H, Watanabe M, Ueda K, Yamato H, Yoshioka T, Motojima M. Uremic toxins overload accelerates renal damage in a rat model of chronic renal failure. *Nephron Exp Nephrol* 2003;**95**:e111–8

18. Lim YJ, Sidor NA, Tonial NC, Che A, Urquhart BL. Uremic toxins in the progression of chronic kidney disease and cardiovascular disease: mechanisms and therapeutic targets. *Toxins* 2021;**13**:142–67

19. Ahmed MSE, Abed M, Voelkl J, Lang F. Triggering of suicidal erythrocyte death by uremic toxin indoxyl sulfate. *BMC Nephrol* 2013;**14**:244

20. Cendoroglo M, Jaber BL, Balakrishnan VS, Perianayagam M, King AJ, Pereira BJ. Neutrophil apoptosis and dysfunction in uremia. *J Am Soc Nephrol* 1999;**10**:93–100

21. Hénaut L, Mary A, Chillon J-M, Kamel S, Massy ZA. The impact of uremic toxins on vascular smooth muscle cell function. *Toxins* 2018;**10**:218–38

22. Shimizu H, Bolati D, Adijiang A, Enomoto A, Nishijima F, Dateki M, Niwa T. Senescence and dysfunction of proximal tubular cells are associated with activated p53 expression by indoxyl sulfate. *Am J Physiol Cell Physiol* 2010;**299**:C1110–7

23. Niwa T, Shimizu H. Indoxyl sulfate induces nephrovascular senescence. *J Ren Nutr* 2012;**22**:102–6

24. Shimizu H, Bolati D, Adijiang A, Muteliefu G, Enomoto A, Nishijima F, Dateki M, Niwa T. NF-κB plays an important role in indoxyl sulfate-induced cellular senescence, fibrotic gene expression, and inhibition of proliferation in proximal tubular cells. *Am J Physiol Cell Physiol* 2011;**301**:C1201–12

25. Kamprom W, Tawonsawatruk T, Mas-Oodi S, Anansilp K, Rattanasompattikul M, Supokawej A. P-cresol and indoxyl sulfate impair osteogenic differentiation by triggering mesenchymal stem cell senescence. *Int J Med Sci* 2021;**18**:744–55

26. Liu Y-x, Dong X, Gong F, Su N, Li S-b, Zhang H-t, Liu J-l, Xue J-h, Ji S-p, Zhang Z-w. Promotion of erythropoietic differentiation in hematopoietic stem cells by SOCS3 knock-down. *PLoS ONE* 2015;**10**:e0135259

27. Wan J, Kalpage HA, Vaishnav A, Liu J, Lee I, Mahapatra G, Turner AA, Zurek MP, Ji Q, Moraes CT, Recanati M-A, Grossman LI, Salomon AR, Edwards BFP, Hüttemann M. Regulation of respiration and apoptosis by cytochrome c threonine 58 phosphorylation. *Sci Rep* 2019;**9**:15815

28. Duangchan T, Tawonsawatruk T, Angsanuntsukh C, Trachoo O, Hongeng S, Kitiyanant N, Supokawej A. Amelioration of osteogenesis in iPSC-derived mesenchymal stem cells from osteogenesis imperfecta patients by endoplasmic reticulum stress inhibitor. *Life Sci* 2021;**278**:119628–43

29. Evenepoel P, Meijers BKI, Bammens BRM, Verbeke K. Uremic toxins originating from colonic microbial metabolism. *Kidney Int Suppl* 2009;**76**:S12–9

30. Wu C-J, Chen C-Y, Lai T-S, Wu P-C, Chuang C-K, Sun F-J, Liu H-L, Chen H-H, Yeh H-I, Lin C-S, Lin C-J. The role of indoxyl sulfate in renal anemia in patients with chronic kidney disease. *Oncotarget* 2017;**8**: 83030–7

31. Fujii H, Goto S, Fukagawa M. Role of uremic toxins for kidney, cardiovascular, and bone dysfunction. *Toxins* 2018;**10**:202–19

32. Yamamoto S, Sasahara K, Domon M, Yamaguchi K, Ito T, Goto S, Goto Y, Narita I. PH-dependent protein binding properties of uremic toxins in vitro. *Toxins* 2021;**13**:116–24

33. Vanholder R, Schepers E, Pletinck A, Nagler EV, Glorieux G. The uremic toxicity of indoxyl sulfate and p-cresyl sulfate: a systematic review. *J Am Soc Nephrol* 2014;**25**:1897–907

34. Lin C-J, Chen H-H, Pan C-F, Chuang C-K, Wang T-J, Sun F-J, Wu C-J. P-Cresylsulfate and indoxyl sulfate level at different stages of chronic kidney disease. *J Clin Lab Anal* 2011;**25**:191–7

35. Yamamoto S, Fuller DS, Komaba H, Nomura T, Massy ZA, Bieber B, Robinson B, Pisoni R, Fukagawa M. Serum total indoxyl sulfate and clinical outcomes in hemodialysis patients: results from the Japan Dialysis Outcomes and Practice Patterns Study. *Clin Kidney J* 2021;**14**:1236–43

36. Dias GF, Bonan NB, Steiner TM, Tozoni SS, Rodrigues S, Nakao LS, Kuntsevich V, Pecoits Filho R, Kotanko P, Moreno-Amaral AN. Indoxyl sulfate, a uremic toxin, stimulates reactive oxygen species production and erythrocyte cell death supposedly by an organic anion transporter 2 (OAT2) and NADPH oxidase activity-dependent pathways. *Toxins* 2018;**10**:280–90

37. Argentati C, Tortorella I, Bazzucchi M, Morena F, Martino S. Harnessing the potential of stem cells for disease modeling: progress and promises. *J Pers Med* 2020;**10**:8–29

38. Bai X. Stem cell-based disease modeling and cell therapy. *Cells* 2020;**9**:2193–200

39. Malik P, Fisher TC, Barsky LLW, Zeng L, Izadi P, Hiti AL, Weinberg KI, Coates TD, Meiselman HJ, Kohn DB. An in vitro model of human red blood cell production from hematopoietic progenitor cells. *Blood* 1998;**91**:2664–71

40. Poldee S, Metheetrairut C, Nugoolsuksiri S, Frayne J, Trakarnsanga K. Optimization of an erythroid culture system to reduce the cost of in vitro production of red blood cells. *MethodsX* 2018;**5**:1626–32

41. Yoshida K, Yoneda T, Kimura S, Fujimoto K, Okajima E, Hirao Y. Polyamines as an inhibitor on erythropoiesis of hemodialysis patients by in vitro bioassay using the fetal mouse liver assay. *Ther Apher Dial* 2006;**10**:267–72

42. Radtke HW, Rege AB, LaMarche MB, Bartos D, Bartos F, Campbell RA, Fisher JW. Identification of spermine as an inhibitor of erythropoiesis in patients with chronic renal failure. *J Clin Invest* 1981;**67**:1623–9

43. Wang W, Liu X, Wang W, Li J, Li Y, Li L, Wang S, Zhang J, Zhang Y, Huang H. The effects of indoxyl sulfate on human umbilical cord-derived mesenchymal stem cells in vitro. *Cell Physiol Biochem* 2016;**38**: 401–14

44. Mathias LA, Fisher TC, Zeng L, Meiselman HJ, Weinberg KI, Hiti AL, Malik P. Ineffective erythropoiesis in beta-thalassemia major is due to apoptosis at the polychromatophilic normoblast stage. *Exp Hematol* 2000;**28**:1343–53

45. Lang F, Bissinger R, Abed M, Artunc F. Eryptosis—the neglected cause of anemia in end stage renal disease. *Kidney Blood Press Res* 2017;**42**: 749–60

46. Ahmed MSE, Langer H, Abed M, Voelkl J, Lang F. The uremic toxin acrolein promotes suicidal erythrocyte death. *Kidney Blood Press Res* 2013;**37**:158–67

47. Föller M, Sopjani M, Mahmud H, Lang F. Vanadate-induced suicidal erythrocyte death. *Kidney Blood Press Res* 2008;**31**:87–93

48. Nicolay JP, Schneider J, Niemoeller OM, Artunc F, Portero-Otin M, Haik G Jr, Thornalley PJ, Schleicher E, Wieder T, Lang F. Stimulation of suicidal erythrocyte death by methylglyoxal. *Cell Physiol Biochem* 2006;**18**:223–32

49. Shamas-Din A, Kale J, Leber B, Andrews DW. Mechanisms of action of Bcl-2 family proteins. *Cold Spring Harb Perspect Biol* 2013;**5**:a008714

50. Esposti MD. The roles of Bid. *Apoptosis* 2002;**7**:433–40

51. Westphal D, Dewson G, Czabotar PE, Kluck RM. Molecular biology of Bax and Bak activation and action. *Biochim Biophys Acta* 2011;**1813**:521–31

52. van Deursen JM. The role of senescent cells in ageing. *Nature* 2014;**509**: 439–46

53. Yi Q, Liu O, Yan F, Lin X, Diao S, Wang L, Jin L, Wang S, Lu Y, Fan Z. Analysis of senescence-related differentiation potentials and gene expression profiles in human dental pulp stem cells. *Cells Tissues Organs* 2017;**203**:1–11

54. Chen H, Liu O, Chen S, Zhou Y. Aging and mesenchymal stem cells: therapeutic opportunities and challenges in the older group. *Gerontology* 2021;**23**:1–14

55. Rufini A, Tucci P, Celardo I, Melino G. Senescence and aging: the critical roles of p53. *Oncogene* 2013;**32**:5129–43

56. González-Gualda E, Baker AG, Fruk L, Muñoz-Espín D. A guide to assessing cellular senescence in vitro and in vivo. *FEBS J* 2021;**288**: 56–80

57. Herranz N, Gil J. Mechanisms and functions of cellular senescence. *J Clin Invest* 2018;**128**:1238–46

58. Adelibieke Y, Shimizu H, Muteliefu G, Bolati D, Niwa T. Indoxyl sulfate induces endothelial cell senescence by increasing reactive oxygen species production and p53 activity. *J Ren Nutr* 2012;**22**:86–9

59. Muteliefu G, Shimizu H, Enomoto A, Nishijima F, Takahashi M, Niwa T. Indoxyl sulfate promotes vascular smooth muscle cell senescence with upregulation of p53, p21, and prelamin A through oxidative stress. *Am J Physiol Cell Physiol* 2012;**303**:C126–34

60. Sardenberg C, Suassuna P, Andreoli MCC, Watanabe R, Dalboni MA, Manfredi SR, dos Santos OP, Kallas EG, Draibe SA, Cendoroglo M. Effects of uraemia and dialysis modality on polymorphonuclear cell apoptosis and function. *Nephrol Dial Transplant* 2006;**21**:160–5

61. Heidenreich S, Schmidt M, Bachmann J, Harrach B. Apoptosis of monocytes cultured from long-term hemodialysis patients. *Kidney Int* 1996;**49**:792–9

62. Majewska E, Baj Z, Sulowska Z, Rysz J, Luciak M. Effects of uraemia and haemodialysis on neutrophil apoptosis and expression of apoptosis-related proteins. *Nephrol Dial Transplant* 2003;**18**:2582–8

63. Soriano S, Martín-Malo A, Carracedo J, Rafael R, Rodriguez M, Aljama P. Lymphocyte apoptosis: role of uremia and permeability of dialysis membrane. *Nephron Clin Pract* 2005;**100**:c71–7

64. Li M, Wang Z, Ma T, Lu G, Yan R, Zhao L, Deng K, Dai K. Enhanced platelet apoptosis in chronic uremic patients. *Ren Fail* 2014;**36**:847–53

65. Crépin T, Legendre M, Carron C, Vachey C, Courivaud C, Rebibou J-M, Ferrand C, Laheurte C, Vauchy C, Gaiffe E, Saas P, Ducloux D, Bamoulid J. Uraemia-induced immune senescence and clinical outcomes in chronic kidney disease patients. *Nephrol Dial Transplant* 2020; **35**:624–32

66. Dussiot M, Maciel TT, Fricot A, Chartier C, Negre O, Veiga J, Grapton D, Paubelle E, Payen E, Beuzard Y, Lebouch P, Ribeil J-A, Arlet J-B, Coté F, Courtois G, Ginzburg YZ, Daniel TO, Chopra R, Sung V, Hermine O, Moura IC. An activin receptor IIA ligand trap corrects ineffective erythropoiesis in β-thalassemia. *Nat Med* 2014;**20**:398–407

67. Voskou S, Aslan M, Fanis P, Phylactides M, Kleanthous M. Oxidative stress in β-thalassaemia and sickle cell disease. *Redox Biol* 2015;**6**: 226–39